SIMULATION AND RECONSTRUCTION OF INTERACTIONS IN THE UPGRADED T2K ND280 NEAR DETECTOR

The 24th International Workshop on Neutrinos from Accelerators
21-26 August 2023, Seoul National University, South Korea

Katharina Lachner on behalf of T2K | WG1x6 Parallel Session | 25 August 2023

WARWICK
THE UNIVERSITY OF WARWICK

Content

The T2K Near Detector Upgrade

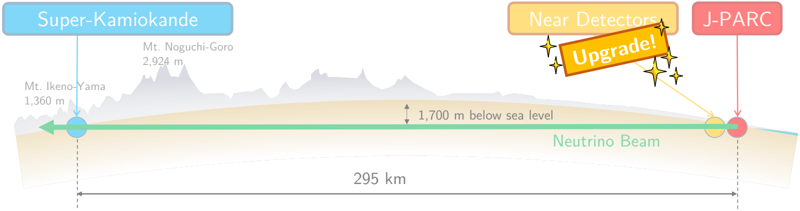

The Off-Axis Near Detector ND280

- Original geometry:

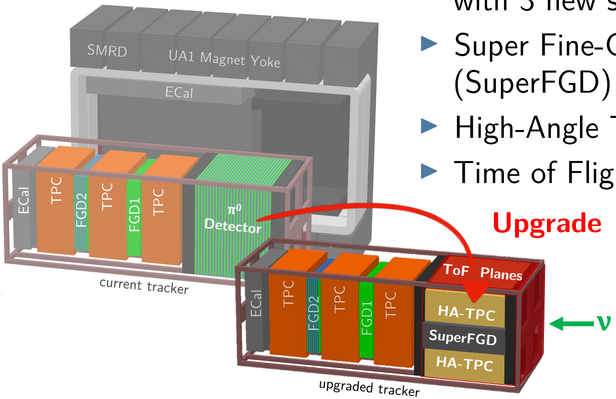

- Replacing the π^0 detector with 3 new sub-detectors
- Super Fine-Grain-Detector (SuperFGD)
- High-Angle TPCs (HA-TPCs)
- Time of Flight planes (ToF)

[1, 2]

SuperFGD and High Angle TPCs

- Polystyrene cubes ($1\,cm^3$)
- Three WLS fibres through each cube ⇒ 3D readout
- High angle & short tracks

- $Ar + CF_4 + iC_4H_{10}$ gas mix
- ERAM[1] readout ($1.1\,cm^2$/pad) ⇒ less channels at higher resolution, spark protection

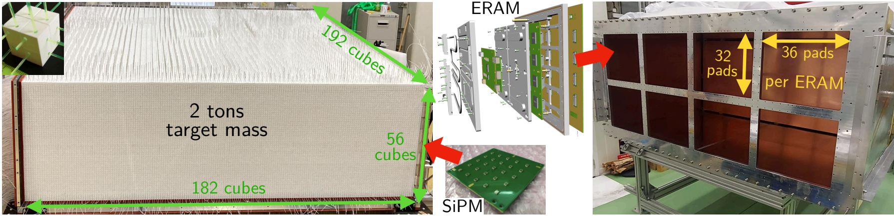

See also D. T. Nguyen's talk

[1]Encapsulated Resistive Anode Micromegas

Simulation

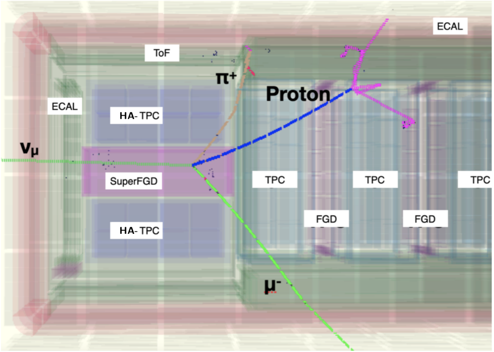

ECAL
ToF
π^+
Proton
ECAL
HA-TPC
ν_μ
SuperFGD
TPC
TPC
TPC
FGD
FGD
HA-TPC
μ^-

Simulation of Neutrino Interactions

- Generate (anti-)ν with *NEUT* generator version 5.4.0 using the *Benhar spectral function* model
- Include quasi elastic scattering, 2p2h, pion production, shallow and deep inelastic scattering
- Nuclear effects, final state int.

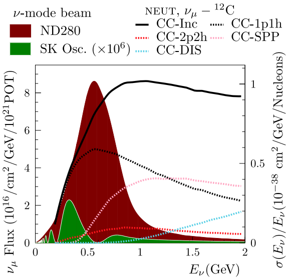

[3]

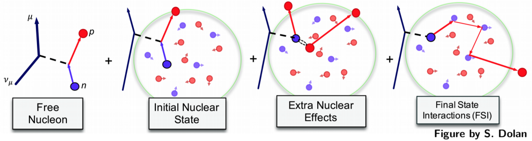

Figure by S. Dolan

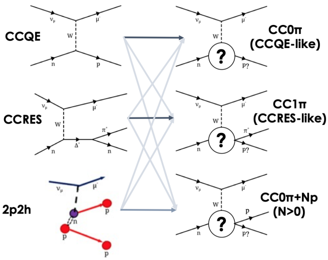

See L. Munteanu and T. Doyle's talks.

Detector Simulation - Overview

- GEANT4: Trajectory in surrounding 0.2 T B-field
- Physics list: *QGSP_BERT* [4]
- Geometry:

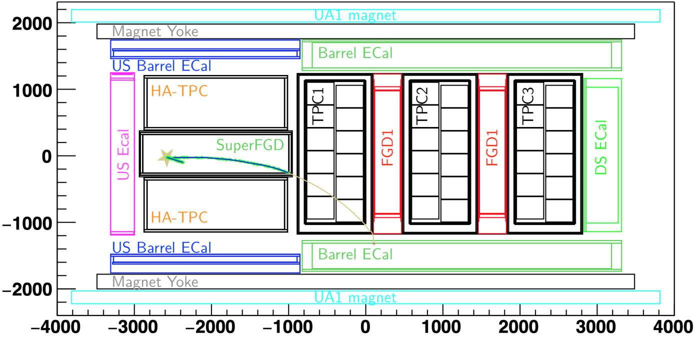

SuperFGD Response Simulation

- Energy deposit (Bethe-Bloch) $\Rightarrow$ scintillation (Birks law)

$$\frac{\mathrm{d}L}{\mathrm{d}x} = \varepsilon_{scint} \cdot \frac{1}{1 + c_B \cdot \mathrm{d}E/\,\mathrm{d}x} \cdot \frac{\mathrm{d}E}{\mathrm{d}x}$$

- Optical cross-talk to adjacent cubes at 3.7% per surface
- WLS fibres, attenuation (463 cm long f. 77%, 33 cm short)
- Collection at SiPMs $\rightarrow$ el. response $\rightarrow$ 0-suppr. (3 p.e.)
- Tuned with test beam data [5], cosmics in progress

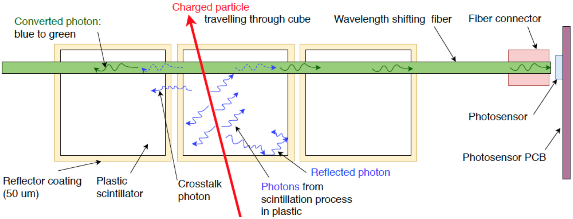

[6]

HA-TPC Response Simulation

- Charge drift in E field following Langevin equation

$$\vec{V}_d = \frac{\mu}{1+(\omega\tau)^2}\left(\vec{E} + \omega\tau\frac{\vec{E}\times\vec{B}}{|\vec{B}|} + (\omega\tau)^2\frac{(\vec{E}\cdot\vec{B})\cdot\vec{B}}{|\vec{B}|^2}\right)$$

- Simulate charge spreading at ERAM readout

$$\rho(\vec{r},t) = \frac{RC}{4\pi t}\cdot\exp\left(-\frac{r^2RC}{4t}\right)$$

and corresponding waveform (as conv. with electronics response)

$$WF(t) = \left(\int_A \rho(\vec{r},t)\,\mathrm{d}x\,\mathrm{d}y\right) \circledast \frac{\mathrm{d}Res_{el}(t)}{\mathrm{d}t}$$

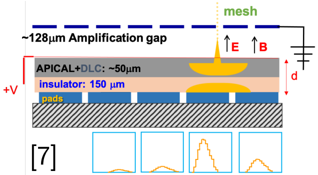

[7]

Reconstruction

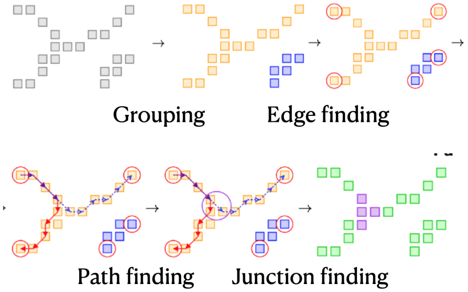

SuperFGD Reconstruction

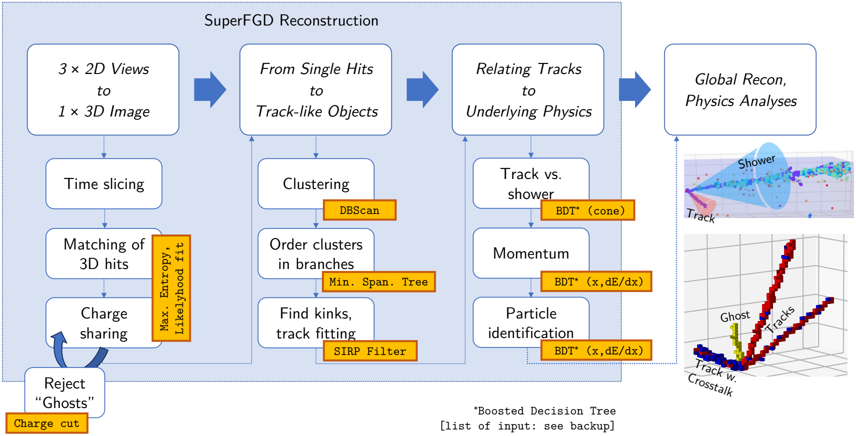

*Boosted Decision Tree
[list of input: see backup]

SuperFGD - Muons (PGun)

Muon momentum resolution for escaping and stopping muons:

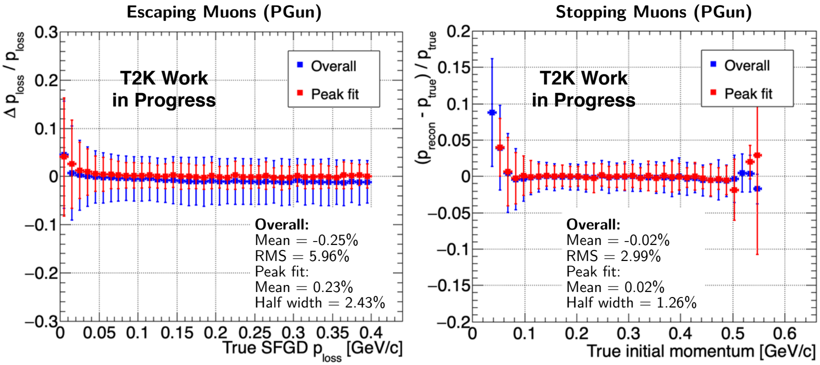

- **Resolution: 6%** (escaping) and **3%** (stopping)

SuperFGD - Protons (PGun)

Momentum (left) and PID (right) for contained protons:

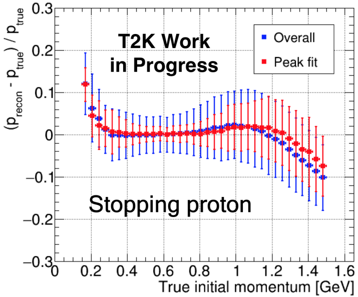

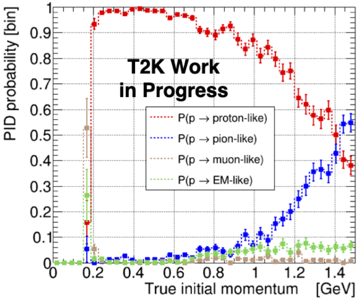

- Excellent resolution at low momenta **down to 300 MeV**
- Momentum threshold for protons in FGDs: 450 MeV [8]

SuperFGD - PID

Confusion matrix for performance of SuperFGD PGun PID:

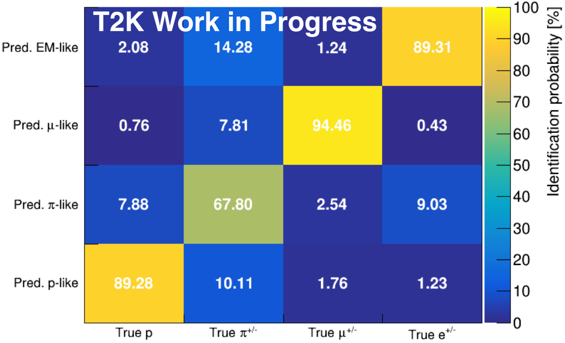

SuperFGD - Shower Identification

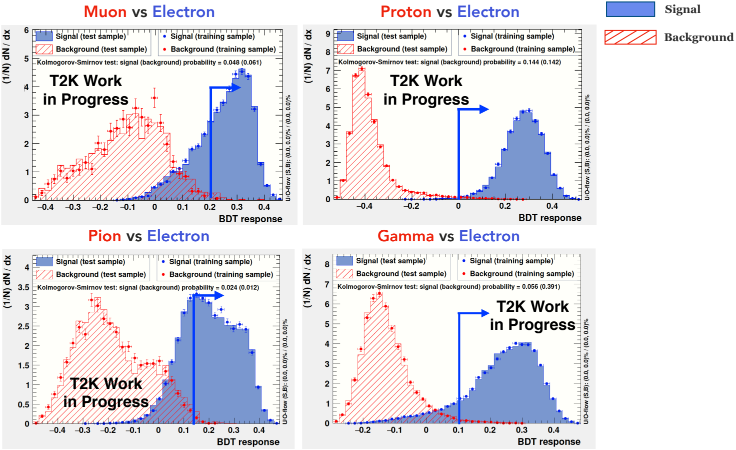

- Excellent separation of e^- vs. γ-induced showers

HA-TPC Reconstruction

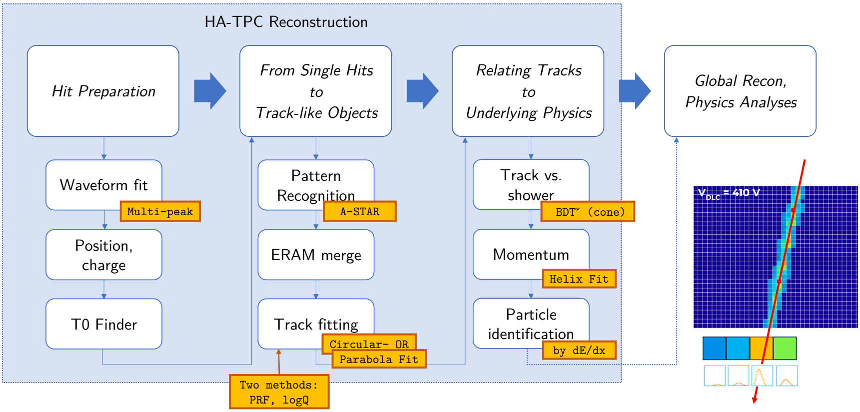

HA-TPC Reconstruction Performance

- PGun events with e^- and μ^- (50 MeV-2.1 GeV)
- PID: pull in dE/dx between measured and expected value

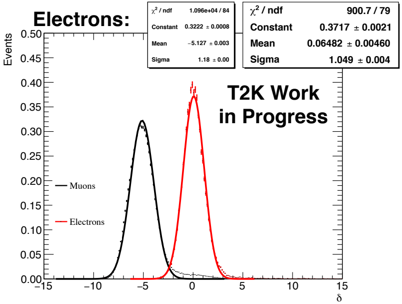

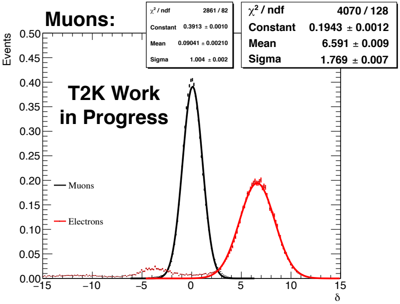

- Spatial resolution **0.45-0.65 mm** (current TPCs 0.6-1 mm)
- dE/dx resolution **7.5±1%** (current TPCs 7.9±0.2%)

Selections and New Variables for Physics Analyses

Selection of $\nu_\mu CC0\pi$ Events

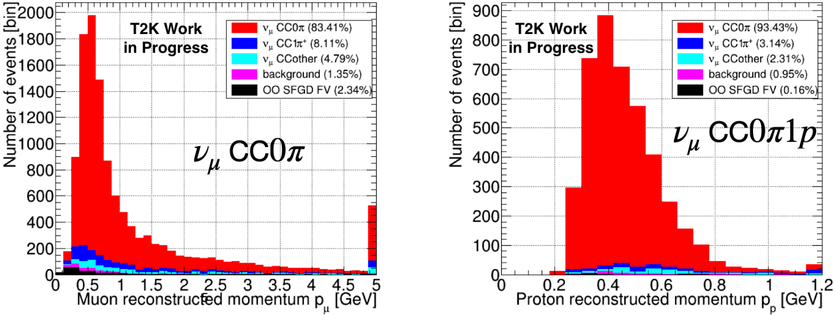

- $\nu_\mu CC0\pi$ **purity 90.8%** (using SuperFGD+vertical TPC)
- $\nu_\mu CC0\pi 1p$ **purity 99.6%** down to **300 MeV protons**
- ν_e selection: ongoing work, currently being validated

Delayed Coincidences in the SuperFGD

- **Neutron** reconstruction from $\bar{\nu}$ via time of flight
- Expected kin. energy resolution around 20% with 70 cm lever arm

[9]

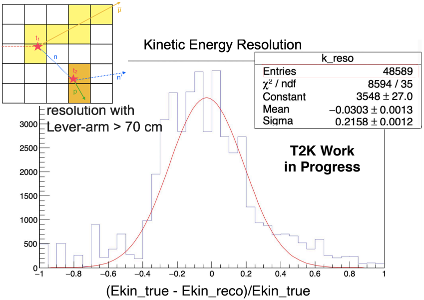

- **Pion** identification and kinematics reconstruction via tagging of delayed Michel e^-
- Without reconstructed π track
- Improved pion selection efficiency at low momentum

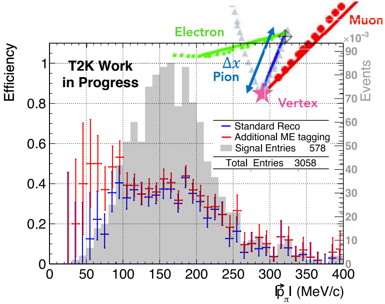

Calorimetric Variables

- Precise calorimetry for *individual* SuperFGD tracks in reconstruction of visible and hadronic energy, vertex activity
- Motivation: good handle on $\sum T_p$ in 0π samples
- Overall resolution on total energy deposit: 1.1% (w.o. syst)
- Developing tools to improve calorimetry for single tracks

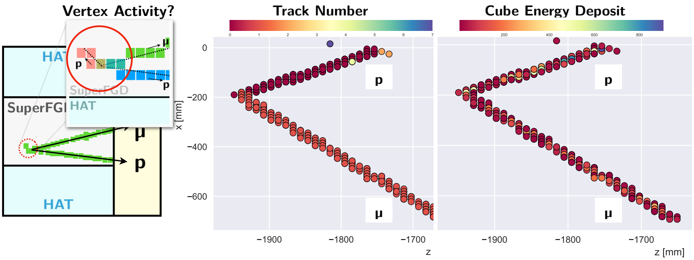

Summary

- Multiple tools for reconstruction of muon- and electron (anti-) neutrinos implemented for SuperFGD&HA-TPCs
  - Work in progress for Time of Flight planes
- Low momentum proton momentum reconstruction and PID works excellent down to 300 MeV
- Selections for ν_μ CC are being finalised, ν_e also on the way
- Exciting new analyses in preparation, including first neutron analysis made possible by the fine granularity
- ND280 upgrade is getting ready for first data this winter!

Thank you for your attention!

Backup - Simulation

Modelling Nuclear Effects and FSI

- Nuclear ground state: Benhar Spectral Function model
- Interaction models:
  - Multi-Nucleon Interactions: Valencia 2p2h
  - Single meson production: Rein-Sehgal with lepton mass corrections for RES and COH
  - Shallow and Deep Inelastic Scattering: GRV98 PDF with Bodek-Yang corrections
- Final state interactions (FSI): cascade models for pion FSI from Salcedo et al., for Nucleon FSI from Bertini et al.

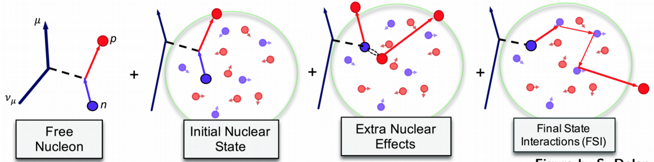

Figure by S. Dolan

Bethe-Bloch Equation

Stopping power in units of energy per density:

$$-\frac{\mathrm{d}E}{\mathrm{d}x} = Kz^2 \frac{Z}{A} \frac{1}{\beta^2} \left[\frac{1}{2} \ln \frac{2 m_e c^2 \beta^2 \gamma^2 W_{max}}{I^2} - \beta^2 - \frac{\delta(\beta\gamma)}{2} \right]$$

Where:

- $K = 4\pi N_A r_e^2 m_e c^2$
- W_{max} ... max. energy transfer to e^-
- I ... mean excitation energy
- $\delta(\beta\gamma)$ ... density correction

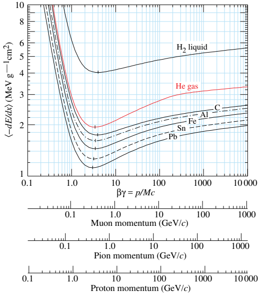

[10]

Density Correction Term $\delta(\beta\gamma)$

Density correction is calculated using Sternheimer parametrisation [11] with constants for polystyrene from [12]:

$$\delta(\beta\gamma) = \begin{cases} 2\ln(10)x + c & \text{if } x \geq x_1 \\ 2\ln(10)x + c + a(x_1 - x)^k & \text{if } x_0 \leq x < x_1 \\ 0 & \text{if } x < x_0 \text{ (nonconductors)} \end{cases}$$

Where:

- $x = \log_{10}(\beta\gamma)$
- $x_0 = 0.1647$
- $x_1 = 2.5031$
- $c = -3.2999$
- $a = 0.16454$
- $k = 3.2224$

Scintillation in the SuperFGD

Apply Birks quenching on each SuperFGD hit-segment's dE/dx:

$$E_{\text{hit}}^{\text{reco}}[p.e.] = corr_{Birks}\left(\mathrm{d}x_n,\ E_n[\text{MeV}] \cdot c_{calib}\right) \times (E_n[\text{MeV}] \cdot c_{calib})$$

...for light yield E_n in p.e. along distance $\mathrm{d}x_n = 10$ mm (one cube), with the following corrections:

- $corr_{Birks}(\mathrm{d}x, E) = \frac{1}{1+ c_B\ E/\,\mathrm{d}x}$, with Birk's constant $c_B = 8.98 \cdot 10^{-3}$ cm/MeV [13]
- Empirical calibration constant $c_{calib} = 320$ p.e./MeV from CERN testbeam data (to be updated when SFGD runs)

SuperFGD Electronics Response

- Apply the effect of the detector (i.e. translate EDepSim output to into hits)
  - Output as calibrated hits
  - "Raw" data produced internally, but not saved
    - Can be saved once SFG electronics/daq is settled
- Structure of simulation
  - Response to Energy
    - Scintillation, saturation, attenuation, transport to sensor, &c
  - Response of Sensors
    - Dark noise, baseline offsets, &c
  - Performance of Electronics
    - Amplification, thresholds, resolutions, &c
  - Structure of DAQ
    - Zero supression, event building, &c
  - Calibration
    - Apply calibration to internally digitized hits.

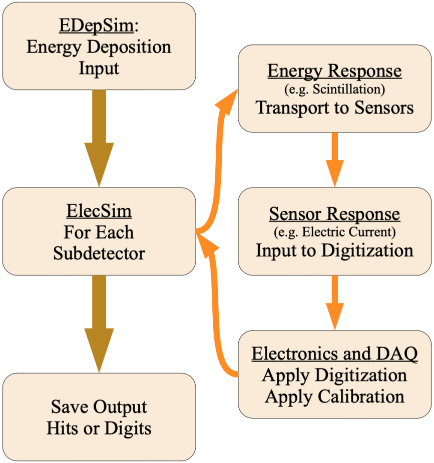

Work by C. McGrew

SuperFGD Test Beam → Sim. Constants

Simulation constants from test beam results:

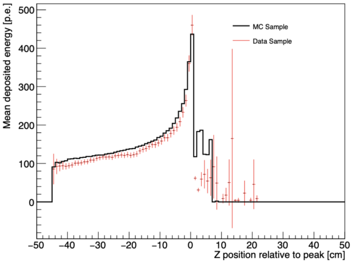

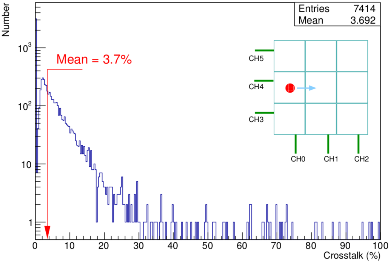

Bragg peak (0.75 GeV protons), Optical cross-talk (6 GeV protons) [5, 14]

ERAM Gain Simulation

Accounting for fluctuations from the calibration result for the gain G (measured per-pad in 55Fe X-Ray scan):

- Each pad's gain is smeared following an exponential distribution
- Corrections for fluctuations in avalanche processes, non-uniformity in the surface etc. are applied
- In particular, each arriving ionisation charge is assigned an effective gain picked from a Polya distribution

ERAM Charge Spreading

Charge in leading vs. neighbouring pad by track position:

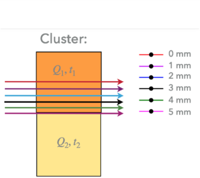

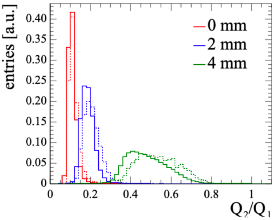

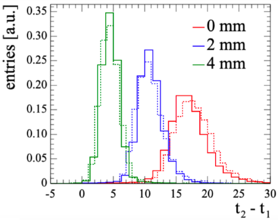

Results from test beam [15]:

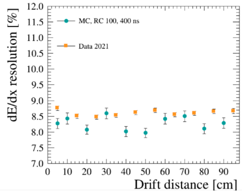

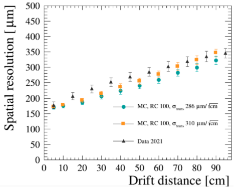

⇒ Data from test beam at DESY 2021 data was reproduced by simulation with RC $= 100\,\mathrm{ns}/\mathrm{mm}^2$

Backup - Reconstruction

SuperFGD Reconstruction

- 3D matching and charge sharing with likelihood fit and entropy maximation
- Reject “ghosts” (shadow tracks) with charge cut and re-apply charge sharing
- Apply clustering algorithm (DBScan)
- Pattern recognition: order hits with minimal spanning tree
- Track fitting with *sequential importance re-sampling particle filter*
- Boosted Decision Tree (BDT) for track mom. and PID: dE/dx per cube position
- BDT for showers: clusters in cone shape from vertex

SuperFGD 3D Matching, Charge Sharing

- 3D matching
  - 3D hit created for every combination of 3 intersecting active fibres within 100 ns
- Charge sharing
  - Likelihood fit for charge sharing: all hit charges have to add up to readout (after attenuation correction)
  - Entropy maximisation ($\sum Q \ln Q$) to avoid degeneracies (priority on higher charges and shorter distances)

SuperFGD Track Fitting

- A *sequential importance re-sampling particle filter* is used for track fitting (very similar to Kalman filter)
  1. High number of random priors
  2. Sequentially update prior with new points (cubes)
  3. Weigh samples (likelihood)
  4. Average sample and repeat
  5. Re-sample posteriors at convergence at weight zero

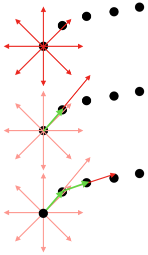

- BDT for track mom. and PID: dE/dx per cube position
- BDT for showers: clusters in cone shape from vertex

BDT for SuperFGD tracks

22 Input parameters:

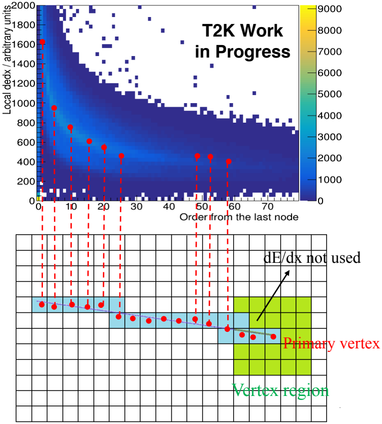

① Node local dE/dx [9]: 3 nodes at the track beginning (after vertex cut) and 6 nodes at the track end.

② Node distance [7]: Distance between two neighboring nodes.

③ dE/dx fluctuation [2]: *(Only for PID)* Mean and standard deviation of dE/dx drop along the track.

④ Total track length [1]: Computed from the first node (without vertex cut).

⑤ Track energy deposition [1]: Computed from the 4^{th} node (with vertex cut).

⑥ Track direction [2]: Polar angle and azimuth angle.

Work by X. Y. Zhao

Muon momentum resolution for SuperFGD

Distribution across full momentum range (backup to slide 13) for escaping (left) and contained tracks (right):

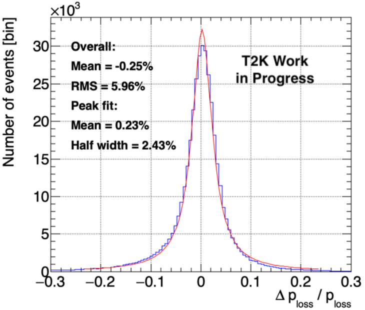

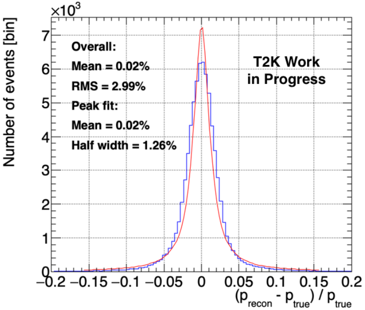

BDT for showers I/II

11 Input variables
- ☑ Number of connected tracks
- ☑ Number of matched tracks
- ☑ Number of matched clusters
- ☑ Length of the primary track
- ☑ dE/dx of the primary track
- ☑ Total energy deposit in cone
- ☑ Axis Max Ratio
- ☑ Truncated Max Ratio
- ☑ Q Root Mean Square
- ☑ Front Back Ratio
- ☑ Maximum Hit Position

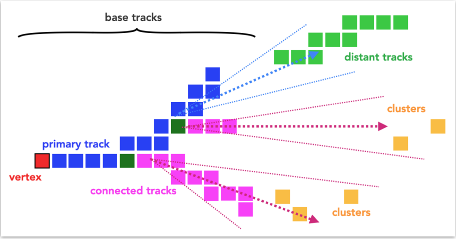

Newly introduced PID variables.
They describe:
- Cone shape
- Hit charge distribution

Trained with particle gun samples.

Work by A. Eguchi

BDT for showers II/II

Axis Max Ratio (AMR)

- Describes cone shape.

Truncated Max Ratio (TMR)

- Charge distribution along the cone axis.

Q Root Mean Square (QRMS)

- RMS of hit charge.

Front Back Ratio (FBR)

- Energy deposit ratio at the front and back of the cone.

Maximum Hit Position (MHP)

- Relative position of the largest charge hit.

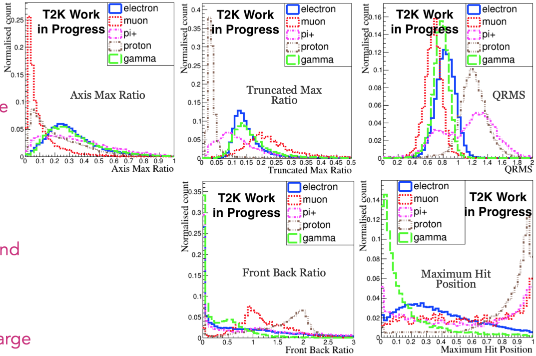

Work by A. Eguchi

Neutrons out of FV

Out of FV background for neutron selection:

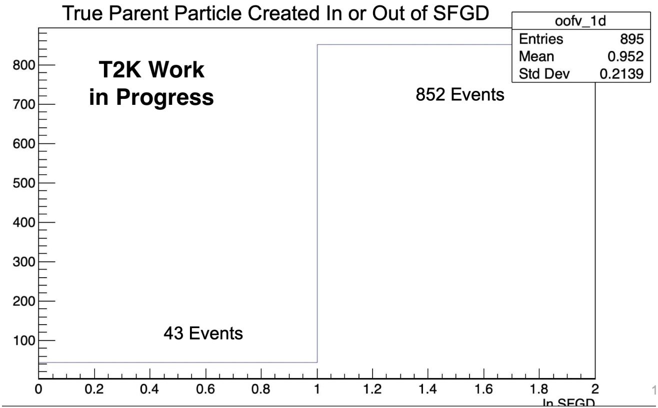

Work by A. Teklu

HA-TPC Reconstruction

- Preparation of hits from fitted waveforms
- Pattern recognition with A-STAR based algorithm
- Position reconstruction per cluster
- Track fitting: circular or parabola fit
- Obtain momentum from helix fit
- PID based on momentum & comparison of measured and expected $\mathrm{d}E/\mathrm{d}x$ for particle hypothesis

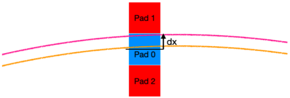

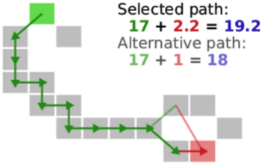

HA-TPC Spatial resolution

Using logQ vs. Pad-Response-Fit (PRF) track fit

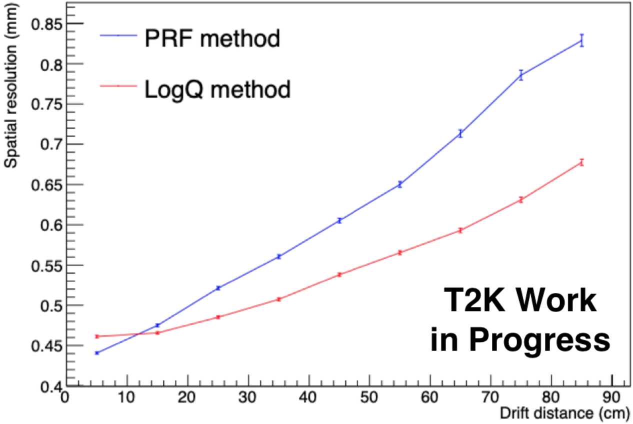

HA-TPC Reconstruction: PID

Pull distributions for e^- vs. μ^- by momentum:

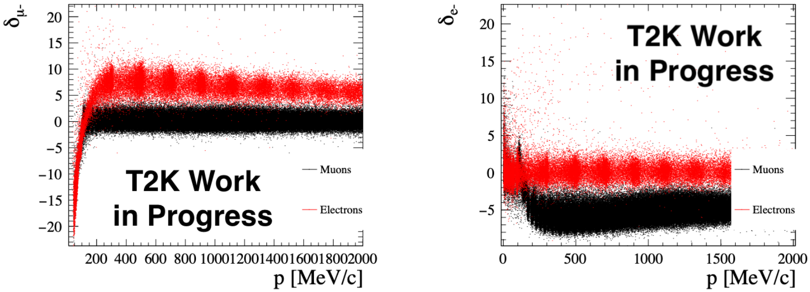

where $\delta_E(i) = \frac{C_T - C_E(i)}{\sigma_E(i)}$

$\Rightarrow 6.6\sigma_E(\mu)$ separation power for muon hypothesis

HA-TPC dE/dx Reconstruction

For vertical electrons and muons, 0.05 GeV/c to 2.1 GeV/c:

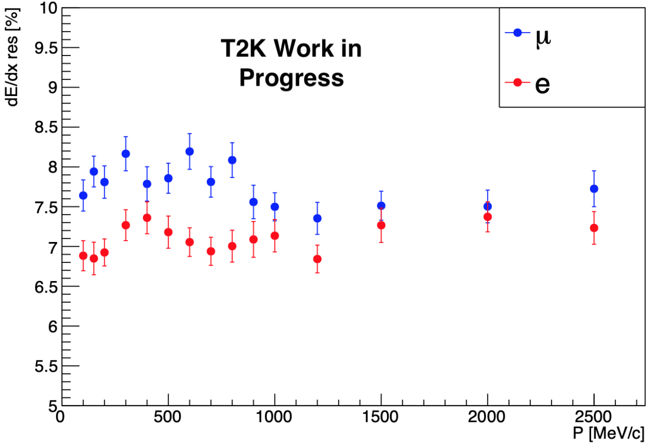

HA-TPC Momentum Reconstruction

Example: muons at 800 MeV:

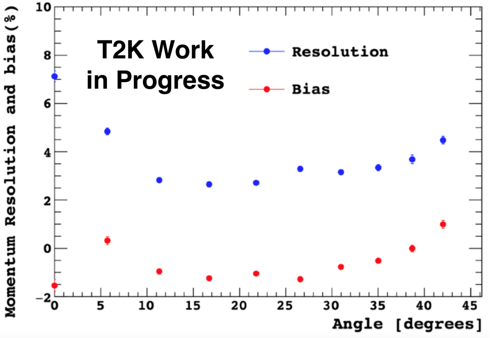

Global Reconstruction

Track matching between sub-detectors $\Rightarrow$ combined momentum:

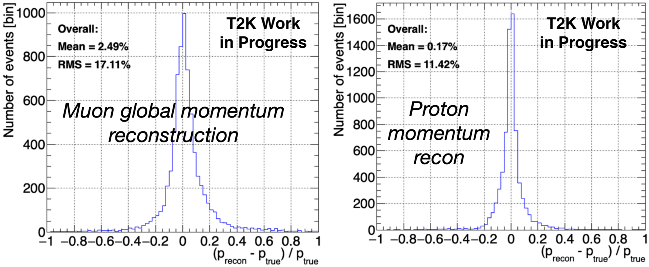

- Global reconstruction for SuperFGD and (vertical) TPC
- Combination with High-Angle TPCs is work in progress

ν_μCC-inclusive Selection Purity

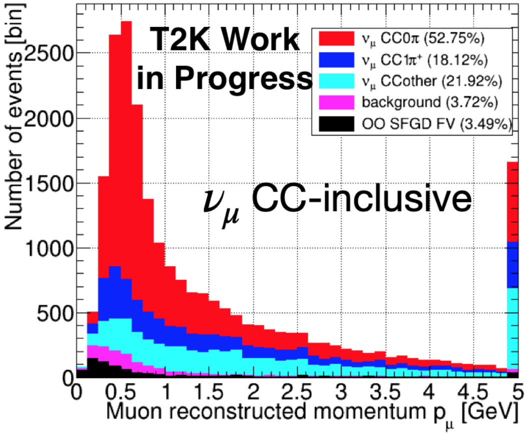

- ν_μCC-incl. purity 94.6%, efficiency 64.7%

References (I)

[1] K. Abe et al. The T2K experiment. *Nuclear Instruments and Methods in Physics Research Section A: Accelerators, Spectrometers, Detectors and Associated Equipment*, 659(1): 106–135, 2011. ISSN 0168-9002. doi: https://doi.org/10.1016/j.nima.2011.06.067. URL `https://www.sciencedirect.com/science/article/pii/S0168900211011910`.

[2] The T2K Collaboration, K. Abe et al. T2K ND280 Upgrade – Technical Design Report, 2020. arXiv:1901.03750 [physics.ins-det].

[3] Ko Abe et al. Improved constraints on neutrino mixing from the t2k experiment with 3.13$\times$ 10 21 protons on target. *Physical Review D*, 103(11):112008, 2021.

References (II)

[4] J. Apostolakis et al. Geometry and physics of the geant4 toolkit for high and medium energy applications. *Radiation Physics and Chemistry*, 78(10):859–873, 2009. ISSN 0969-806X. doi: https://doi.org/10.1016/j.radphyschem.2009.04.026. URL https://www.sciencedirect.com/science/article/pii/S0969806X09001650.

[5] A. Blondel et al. The SuperFGD prototype charged particle beam tests. *Journal of Instrumentation*, 15(12):P12003–P12003, dec 2020. doi: 10.1088/1748-0221/15/12/p12003. URL https://doi.org/10.1088%2F1748-0221%2F15%2F12%2Fp12003.

[6] A Blondel, F Cadoux, S Fedotov, M Khabibullin, A Khotjantsev, A Korzenev, A Kostin, Y Kudenko, A Longhin, A Mefodiev, et al. A fully-active fine-grained detector with three readout views. *Journal of Instrumentation*, 13(02):P02006, 2018.

References (III)

[7] D. Attie et al. Characterization of charge spreading and gain of encapsulated resistive micromegas detectors for the upgrade of the t2k near detector time projection chambers, 2023.

[8] Ko Abe et al. Characterization of nuclear effects in muon-neutrino scattering on hydrocarbon with a measurement of final-state kinematics and correlations in charged-current pionless interactions at t2k. *Physical Review D*, 98(3):032003, 2018.

[9] L Munteanu, S Suvorov, S Dolan, D Sgalaberna, S Bolognesi, S Manly, G Yang, C Giganti, K Iwamoto, and C Jesús-Valls. New method for an improved antineutrino energy reconstruction with charged-current interactions in next-generation detectors. *Physical Review D*, 101(9):092003, 2020.

References (IV)

[10] Particle Data Group (P A Zyla et al.). Review of Particle Physics. *Progress of Theoretical and Experimental Physics*, 2020(8), 08 2020. ISSN 2050-3911. doi: 10.1093/ptep/ptaa104. URL https://doi.org/10.1093/ptep/ptaa104. 083C01.

[11] R. M. Sternheimer. The density effect for the ionization loss in various materials. *Phys. Rev.*, 88:851–859, Nov 1952. doi: 10.1103/PhysRev.88.851. URL https://link.aps.org/doi/10.1103/PhysRev.88.851.

[12] R.M. Sternheimer, M.J. Berger, and S.M. Seltzer. Density effect for the ionization loss of charged particles in various substances. *Atomic Data and Nuclear Data Tables*, 30(2):261–271, 1984. ISSN 0092-640X. doi: https://doi.org/10.1016/0092-640X(84)90002-0. URL https://www.sciencedirect.com/science/article/pii/0092640X84900020.

References (V)

[13] M Hirschberg, R Beckmann, U Brandenburg, H Bruckmann, and K Wick. Precise measurement of birks kb parameter in plastic scintillators. *IEEE Transactions on Nuclear Science*, 39(4):511–514, 1992.

[14] O Mineev, A Blondel, Y Favre, S Fedotov, A Khotjantsev, A Korzenev, Yu Kudenko, A Mefodiev, E Noah, D Sgalaberna, et al. Beam test results of 3d fine-grained scintillator detector prototype for a t2k nd280 neutrino active target. *Nuclear Instruments and Methods in Physics Research Section A: Accelerators, Spectrometers, Detectors and Associated Equipment*, 923:134–138, 2019.

References (VI)

[15] D. Attié et al. Analysis of test beam data taken with a prototype of TPC with resistive micromegas for the t2k near detector upgrade. *Nuclear Instruments and Methods in Physics Research Section A: Accelerators, Spectrometers, Detectors and Associated Equipment*, 1052:168248, jul 2023. doi: 10.1016/j.nima.2023.168248. URL `https://doi.org/10.1016%2Fj.nima.2023.168248`.